

# 1-2-1: Renaissance of Single-Network Paradigm for Virtual Try-On

Shuliang Ning<sup>1,2</sup>   Yipeng Qin<sup>3</sup>   Xiaoguang Han<sup>2,1,\*</sup>  
<sup>1</sup> FNii, CUHKSZ   <sup>2</sup> SSE, CUHKSZ   <sup>3</sup> Cardiff University



Figure 1. Examples of image and video virtual try-on (VTON) results on VITONHD [2] and VIVID [5] datasets. (a): Warping-based Try-On; (b): ReferenceNet-based Try-On; (c) MN-VTON (Ours). Our MN-VTON marks a renaissance of the *single-network paradigm* for VTON used in (a) but discarded in (b). The rest of the figure shows the results of our MN-VTON for both image and video VTON.

## Abstract

Virtual Try-On (VTON) has become a crucial tool in e-commerce, enabling the realistic simulation of garments on individuals while preserving their original appearance and pose. Early VTON methods relied on **single** generative networks, but challenges remain in preserving fine-grained garment details due to limitations in feature extraction and fusion. To address these issues, recent approaches have

adopted a **dual-network paradigm**, incorporating a complementary “ReferenceNet” to enhance garment feature extraction and fusion. While effective, this dual-network approach introduces significant computational overhead, limiting its scalability for high-resolution and long-duration image/video VTON applications. In this paper, we challenge the dual-network paradigm by proposing a novel **single-network VTON** method that overcomes the limitations of existing techniques. Our method, namely MN-VTON, introduces a Modality-specific Normalization strat-

\* Corresponding Author.

egy that separately processes text, image and video inputs, enabling them to share the same attention layers in a VTON network. Extensive experimental results demonstrate the effectiveness of our approach, showing that it consistently achieves higher-quality, more detailed results for both image and video VTON tasks. Our results suggest that the single-network paradigm can rival the performance of dual-network approaches, offering a more efficient alternative for high-quality, scalable VTON applications.

## 1. Introduction

Virtual Try-On (VTON) enables the seamless alteration of a person’s clothing in an image or video, allowing different garments to be realistically simulated while preserving the individual’s original appearance and pose [9, 15]. As e-commerce expands and demand for personalized shopping grows, VTON has become a vital tool in online retail. For merchants, it enables showcasing multiple garments on the same model without costly photoshoots, simplifying inventory and enhancing visual appeal. Meanwhile, AI-driven VTON also appeals to casual users, allowing them to explore styles interactively and create engaging content.

Early methods [2, 9, 15, 23, 26, 35, 39] laid the groundwork for image-based VTON by employing a **single** generative network to synthesize realistic results. These methods leverage the capabilities of deep generative models, such as GANs [7], by first warping the garment to align with the target person’s pose, and then blending the warped garment onto the target person’s image using a generative network. However, recognizing that the features of warped garment images can be “washed away” during network propagation [19], researchers proposed layer-wise conditioning techniques that incorporate additional garment features throughout the generation process, significantly advancing VTON results [8, 17]. For instance, LaDI-VTON [17] utilizes a CLIP [21] encoder to extract features from both the garment image and its textual description, using these as conditioning inputs to enhance realism in the generated results. Despite these advancements, single-network methods still face challenges in preserving fine-grained garment textures, largely due to three inherent limitations:

- [L1] CLIP is designed for high-level semantic representation, often neglecting the subtle textural details crucial for garment realism.
- [L2] Applying the same generalized CLIP features uniformly across all layers fails to account for the unique characteristics of each layer, resulting in a mismatch.
- [L3] CLIP handles text and image inputs similarly, neglecting the intrinsic differences between the visual and textual modalities, resulting in suboptimal fusion and texture preservation.

State-of-the-art methods [3, 14, 28, 33, 40, 41] address

these three limitations with a **dual** networks paradigm, which introduces a complementary *ReferenceNet* with the same architecture as the main generative network. Specifically, this *ReferenceNet* addresses [L1] by being trainable, allowing it to learn and extract the textual details crucial for VTON; [L2] by extracting multi-level features from the garment image and feeding them into the corresponding layers of the main generative network, respectively; and [L3] by using only the garment image as input, which ensures a single-modality, focused feature extraction process. This paradigm has also been adopted by state-of-the-art video VTON methods [5, 30, 36], which extend image-based VTON approaches by incorporating temporal attention modules to ensure continuity and coherence across video sequences. To date, the *dual-network paradigm* to extract garment features has become a **common belief** in VTON. However, while effective, the inclusion of an additional *ReferenceNet* introduces substantial computational overhead. This becomes an increasingly significant concern as user demands for higher-resolution, greater-fidelity, and longer-duration images and videos continue to grow, posing a major challenge for the practical deployment of such methods in real-world scenarios.

In this paper, we challenge the above-mentioned belief by proposing a novel method, namely MN-VTON, which achieves high-quality VTON with a **single** generative network, marking a renaissance of *single-network paradigm* for VTON. Specifically, we address [L3] by introducing a novel Modality-specific Normalization strategy that normalizes and modulates different input modalities (text, image/video) separately, enabling them to be effectively processed by the *same* attention layer; [L2] by nature as the features extracted at each layer correspond to its specific characteristics; and [L1] by nature as the network layers are trainable, allowing them to learn and extract the textual details crucial for VTON. Extensive experiments on two image datasets (VITONHD [2], DressCode [16]) and two video datasets (VVT [25], VIVID [5]) demonstrate the effectiveness of our method. Our contributions include:

- We challenge the *dual network paradigm* belief in VTON and propose a novel method that achieves high-quality VTON with a *single* network, marking a renaissance of *single-network paradigm* for VTON (*i.e.*, 1-2-1).
- We propose a novel modality-specific normalization strategy that normalizes and modulates different input modalities (text, image/video) separately, enabling them to be effectively processed by the *same* attention layers.
- Extensive experiments demonstrate that our method consistently delivers higher quality and more detailed results for image VTON tasks, as well as higher fidelity and higher resolution for video VTON tasks.



## 2. Related Work

**Single-Network Virtual Try-On.** Image-based virtual try-on (VTON) methods aim to generate realistic images of a person wearing a specified garment while preserving the individual’s original pose and identity. Early approaches established the foundation for VTON by utilizing a **single** generative network to synthesize lifelike try-on results. These early models employed techniques ranging from feed-forward warping networks [6, 9, 24, 27] to diffusion-based iterative sampling [4, 13, 18, 29, 31, 34, 40], each contributing essential advancements toward realistic and reliable VTON experiences. Specifically, warping-based methods are typically divided into two stages: a clothing warping network that adapts the garment to fit the person’s body shape, and a generative try-on network that seamlessly blends the warped clothing with the human model. Notably, VITON [9] first introduced the use of the Thin Plate Spline (TPS) transformation to effectively deform clothing to fit the target body. Building on this, CP-VTON [24] refined the VTON process by explicitly dividing it into warping and generation stages, enhancing control over garment fit and appearance. More recently, GP-VTON [39] proposed the Local-Flow Global-Parsing (LFGP) warping module, achieving semantically accurate garment deformation even with challenging inputs. With the advent of diffusion models, researchers have explored these as replacements for traditional feed-forward networks as the try-on module. Both [8, 17] integrate warping modules with diffusion-based try-on networks, producing high-quality, realistic try-on results that significantly enhance visual fidelity. In addition, [17] recognizes that the features of warped garment images can be “washed away” during network propagation [19] and proposed a CLIP-based layer-wise conditioning technique that incorporates additional garment features throughout the generation process to improve VTON results.

Despite these advancements, single-network methods face three key limitations ([L1], [L2], and [L3]) as outlined in Sec. 1, which have driven the development of the dual-network paradigm for VTON.

**Dual-Network Virtual Try-On.** TryOnDiffusion [40] first introduces a garment encoder that extracts clothing features and employs cross-attention mechanisms to merge the garment and person features, enabling implicit warping and try-on of clothes. Building on [40] and [10], recent methods [3, 14, 28, 33] leverage a **dual**-network paradigm, which either fully or partially replicates the original U-Net structure. Experiments with these approaches demonstrate that the use of well-aligned, multi-scale features significantly improves the detail and realism of generated clothing. In addition, this dual-network paradigm has proven effective not only for image-based VTON but also for video VTON, where it is further enhanced by incorporating a temporal attention

module to capture and model temporal shifts in the video.

However, the inclusion of an additional network introduces significant computational overhead. As the demand for higher-resolution, higher-fidelity, and longer-duration images and videos continues to grow, the limitations of dual-network methods have become increasingly apparent.

**Video Generation and Virtual Try-On.** The marriage of video generation and video virtual try-on (VTON) begins with a paradigm where the initial image is generated by a try-on network [22], followed by the generation of the full video using pose-guided video diffusion models [11]. This approach primarily emphasizes maintaining body consistency across frames, with less focus on garment details. Subsequent works [5, 30] have enhanced this paradigm by incorporating the try-on functionality directly into pose-guided video generation, creating end-to-end systems. While these methods show promising results, they may struggle with vigorous human motion and complex garment textures. Despite employing a temporal module across the time dimension, it often functions as a local attention mechanism within the spatial region. Recent advancements in text-to-video generation [32, 38] highlight the effectiveness of DiT [20] and full attention mechanisms across both temporal and spatial dimensions. This 3D full attention approach ensures that all pixels in a sequence of feature maps contribute to the attention map, enabling smooth and coherent motion even in the presence of vigorous movement.

Our approach diverges from some concurrent works [37] by unifying the image and video VTON within a single framework, eliminating the need for an additional network.

## 3. Method

As discussed in Sec. 1, state-of-the-art methods address the three limitations [L1], [L2], [L3] of early single-network methods with a novel **dual** network paradigm. In this work, we challenge this paradigm by showing that i) [L1] and [L2] can be effectively mitigated through a novel layer-wise feature split, normalization, and fusion strategy (Sec. 3.2); ii) [L3] can be addressed by a novel modality-specific normalization technique (Sec. 3.3). Both techniques are implemented within a single network.

### 3.1. Preliminaries

Given a person image/video  $I$  and a reference garment  $G$ , our goal is to generate a new image/video  $\hat{I}$  that preserves the original pose and identity of the person while seamlessly replacing their outfit with the reference garment.

**Single-Network Paradigm.** As discussed earlier, single-network methods typically rely on a warping module to adjust the clothing to fit the human body, which can be formu-

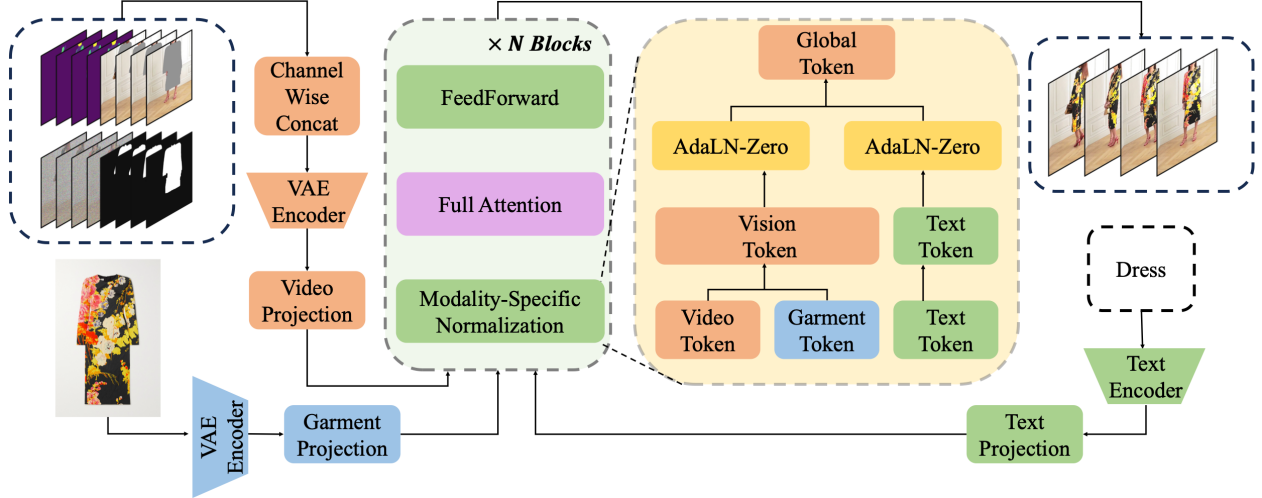


Figure 2. Overview of the proposed MN-VTON. Our method achieves high-quality image and video virtual try-on (VTON) through a Modality-Specific Normalization module. Specifically, for multi-modal inputs, we first apply identical AdaLN-zero normalization for similar modality inputs (e.g., reference garment and image/video) and distinct AdaLN-zero normalization for different modalities (e.g., text and visual inputs). Next, we employ shared-weight self-attention across all tokens to enable effective VTON using only a *single* network.

lated as follows:

$$\hat{I} = \text{VTON}(I_m, M, P, G_w, C_{text}, C_{garment}) \quad (1)$$

where  $I_m$  represents the clothing-agnostic version of the input person image/video  $I$ ;  $M$  denotes the garment inpainting mask;  $P$  denotes the human pose;  $G_w$  is the warped garment, typically generated by a garment warping module;  $C_{text}$  and  $C_{garment}$  are layer-wise CLIP features extracted from the input descriptive text and garment image  $G$ , respectively. Note that conventional methods do not use  $C_{text}$  and  $C_{garment}$  and primarily focus on blending the warped garment onto the person. Nevertheless, recent diffusion-based approaches, such as LaDI-VTON [17], show that incorporating  $C_{text}$  and  $C_{garment}$  mitigates the feature “wash-away” effect during network propagation [19] and is beneficial for VTON.

**Dual-Network Paradigm.** To further refine the details of the clothing, an additional *ReferenceNet* is employed to extract well-aligned, multi-scale garment features. These features are then integrated with the person’s features using a self-attention mechanism, which can be formulated as:

$$\mathbf{F}^{\text{ref}} = \{F_0^{\text{ref}}, F_1^{\text{ref}}, \dots, F_N^{\text{ref}}\} = \text{ReferenceNet}(G) \quad (2)$$

$$\hat{I} = \text{VTON}(I_m, M, P, C_{text}, \mathbf{F}^{\text{ref}})$$

where  $\mathbf{F} = \{F_0, F_1, \dots, F_N\}$  is the layer-wise features extracted by *ReferenceNet*,  $N$  is the number of layers.

**Remark.** It is important to highlight that pose plays a critical and irreplaceable role in VTON. Specifically, like the third line of Fig. 4, when a person’s upper body is occluded or masked, pose information is essential for accurately reconstructing the body and ensuring a realistic garment fit.

### 3.2. Feature Split, Normalization and Fusion

As Eq. 2 shows, dual-network methods address the limitations of [L1] and [L2] by introducing an additional *ReferenceNet*. This network not only extracts multi-scale garment features but also seamlessly fuses them with those from the *Main Network* for further processing. Let  $\mathbf{F}^{\text{main}} = \{F_0^{\text{main}}, F_1^{\text{main}}, \dots, F_N^{\text{main}}\}$  be the features of the Main Network, dual-network methods proposed that:

$$\begin{aligned} Q^l &= W_Q^l F_l^{\text{main}} \\ K^l &= W_K^l [F_l^{\text{main}} \oplus F_l^{\text{ref}}] \\ V^l &= W_V^l [F_l^{\text{main}} \oplus F_l^{\text{ref}}] \\ F_{l+1}^{\text{main}} &= \text{Attention}(Q^l, K^l, V^l) \end{aligned} \quad (3)$$

where  $\oplus$  denotes feature concatenation along the channel axis;  $l$  is the layer ID.

However, the feature extraction and fusion strategy in Eq. 3 presents a challenge for single-network methods, as their network layers output only a single feature  $F_l^{\text{main}}$ . To address this issue, a straightforward approach is to introduce a *split-and-fusion* strategy, which splits  $F_l^{\text{main}}$  into two parts:  $F_l^{\text{main},1}$  and  $F_l^{\text{main},2}$  ( $F_l^{\text{main}} = F_l^{\text{main},1} \oplus F_l^{\text{main},2}$ ), and processes them similarly to  $F_l^{\text{main}}$  and  $F_l^{\text{ref}}$  in Eq. 3, respectively:

$$\begin{aligned} Q^l &= W_Q^l F_l^{\text{main},1} \\ K^l &= W_K^l [F_l^{\text{main},1} \oplus F_l^{\text{main},2}] \\ V^l &= W_V^l [F_l^{\text{main},1} \oplus F_l^{\text{main},2}] \\ F_{l+1}^{\text{main}} &= \text{Attention}(Q^l, K^l, V^l) \end{aligned} \quad (4)$$

Nevertheless, this approach has two major problems: i) *feature shrinking*: the dimension of  $Q^l/F_l^{\text{main},1}$  is smaller than

$F_l^{\text{main}}$ , resulting in the dimension of  $F_{l+1}^{\text{main}} < F_l^{\text{main}}$ ; ii) since  $F_l^{\text{main},1} \oplus F_l^{\text{main},2} = F_l^{\text{main}}$ , Eq. 4 is not effective as it is essentially a weaker version of the native single-attention mechanism where  $Q^l = W_Q^l[F_l^{\text{main},1} \oplus F_l^{\text{main},2}]$ . To alleviate these problems, we have modified Eq. 4 by introducing separate normalization layers for  $F_l^{\text{main},1}$  and  $F_l^{\text{main},2}$ , respectively, and use both of them in  $Q$ , and have:

$$\begin{aligned} F_l' &= \text{Norm}(F_l^{\text{main},1}) \oplus \text{Norm}(F_l^{\text{main},2}) \\ Q^l &= W_Q^l F_l', K^l = W_K^l F_l', V^l = W_V^l F_l' \\ F_{l+1}^{\text{main}} &= \text{Attention}(Q^l, K^l, V^l) \end{aligned} \quad (5)$$

where  $F_l' \neq F_l^{\text{main}}$  as  $F_l^{\text{main},1}$  and  $F_l^{\text{main},2}$  are modulated independently based on their distinct characteristics, thereby effectively capturing the advantages of Eq. 3. However, the effectiveness of Eq. 5 depends on the splitting strategy of  $F_l^{\text{main},1}$  and  $F_l^{\text{main},2}$ , which will be discussed in-depth in the following subsection.

### 3.3. Modality-Specific Normalization

As mentioned above, the splitting strategy of  $F_l^{\text{main},1}$  and  $F_l^{\text{main},2}$  plays a key role in the success of our method. Similar to previous works [28], our method also takes three inputs: i) *Text*, which describes the type of garment (e.g., upper-body, lower-body, dress); ii) *Garment Image*, which is the garment to be worn on the target person; iii) *Target Image/Video*, which contains the target person who will wear the garment. Therefore, we propose to split  $F_l^{\text{main},1}$  and  $F_l^{\text{main},2}$  according to their modalities and apply normalization to them separately, namely Modality-Specific Normalization, which addresses the limitation [L3]. Specifically, as Fig. 2 (d) shows, we propose that:

$$\begin{aligned} F_l^{\text{main},1} &= F_l^{\text{text}} \\ F_l^{\text{main},2} &= F_l^{\text{garment}} \oplus F_l^{\text{target}} \end{aligned} \quad (6)$$

where  $F_l^{\text{text}}$ ,  $F_l^{\text{garment}}$ , and  $F_l^{\text{target}}$  denote the respective feature components of  $F_l^{\text{main}}$  corresponding to the text, garment image, and target image or video modalities, respectively. The rationale for this is from several key insights:

- Normalization preserves the relative relationships between different modalities in a multimodal distribution.
- Retaining garment and target image or video information throughout the network is essential to capture fine-grained details.
- Text information provides complementary semantic context for VTON task.

Thus, concatenating  $F_l^{\text{garment}}$  and  $F_l^{\text{target}}$  while processing  $F_l^{\text{text}}$  separately is the most effective approach. To support this, we visualize the garment feature maps  $F_l^{\text{garment}}$  using Principal Component Analysis (PCA) for two different splitting strategies in Fig. 3. It shows that combining mismatched modalities, such as  $F_l^{\text{text}}$  and  $F_l^{\text{garment}}$ , introduces

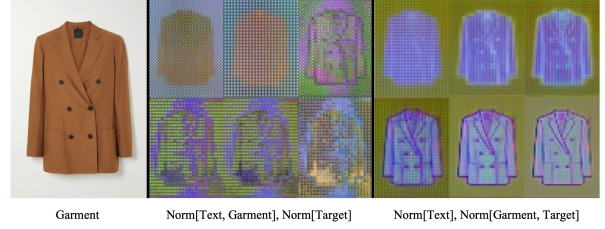


Figure 3. Visualization of garment feature maps  $F_l^{\text{garment}}$  using PCA at the output of blocks 1, 6, 11, 16, 21, 26 of our MN-VTON.  $[\cdot, \cdot]$  denotes different combinations of input modalities.

Methods	SSIM $\uparrow$	LPIPS $\downarrow$	Trainable Param.
Reference-UNet	0.8756	5.412	1700.25M
Ours (UNet)	0.8768	5.357	859.57M
Ours (DiT)	0.8879	0.0632	1694.28M

Table 1. Generalization ability of our method across architectures.

blurriness and artifacts in the garment features, whereas aligning similar modalities, like  $F_l^{\text{garment}}$  and  $F_l^{\text{target}}$ , produces garment features that are both clear and informative.

**Remark.** Another straightforward approach would be to split and normalize each of the three modalities independently. However, as discussed earlier, the Garment Image and Target Image/Video share similar characteristics, and separating them does not yield additional benefits. Please see the supplementary materials for more details.

### 3.4. Image-Video Joint training Strategy

We trained our VTON model on two image datasets and one video dataset (VIVID [5]) for high quality video generation. The image datasets provide a diverse set of cloth-person identities, enhancing generalization, while the video dataset enables the model to learn temporal coherence. Specifically, we applied position embedding interpolation [1] to align position encodings between image and video inputs, allowing both to share a common position encoding. This approach improves the model’s ability to generate fine clothing details while preserving temporal consistency across frames.

## 4. Experiment

### 4.1. Experimental Setup

**Datasets & Implementation Details.** Two image datasets (VITONHD [2], DressCode [16]) and two video datasets (VVT [25], VIVID [5]) are used for evaluation. Our model is trained based on Cogvideo-2B [32]. For image VTON task, in order to ensure a fair comparison, we independently trained two models specifically for the VITONHD and DressCode datasets. Each model was then evaluated on its respective test set, consistent with the approach adopted by previous methods. The training and testing resolution are  $1,024 \times 768$ , and then all images are resized two  $512 \times 384$





Figure 4. Visual comparison on the VITONHD dataset. Please zoom in for more details.



Figure 5. Visual Comparison on VVT dataset.

for metric evaluation. All image related experiments were conducted on 8 Nvidia A100 GPUs. We set the learning rate to  $2e-4$ , utilized the AdamW optimizer, and trained with a batch size of 64 for 16,000 steps. For video VTON task, a clip of 25 frames is used as the video input. The training resolution is  $512 \times 384$  for VIVID [5] dataset and  $256 \times 192$  for VVT [25] dataset. All video models use hyper-parameters similar to the image models, but the batch size and training steps are adjusted to 16 and 20,000 respectively.

#### 4.2. Generalization across Network Architectures

To validate the generalization of our method across network architectures, we conducted experiments on the following

three methods: i) original ReferenceNet-based diffusion UNet. ii) diffusion UNet with our Modality-specific Normalization (ReferenceNet-free); iii) DiT with our Modality-specific Normalization (ReferenceNet-free). As shown in Table 1, by eliminating ReferenceNet and concatenating the features of the garment and target images along the token dimension, Ours (UNet) can achieve results comparable to those of ReferenceNet while significantly reducing the trainable parameters; while Ours (DiT) uses a similar number of trainable parameters but significantly outperforms ReferenceNet. Without loss of generality, we chose DiT for our MN-VTON from its superior performance, and use it for all the following experiments.

Method	VTIONHD						DressCode					
	Paired				Unpaired		Paired				Unpaired	
	SSIM $\uparrow$	FID $\downarrow$	KID $\downarrow$	LPIPS $\downarrow$	FID $\downarrow$	KID $\downarrow$	SSIM $\uparrow$	FID $\downarrow$	KID $\downarrow$	LPIPS $\downarrow$	FID $\downarrow$	KID $\downarrow$
DCI-VTON[8]	0.8620	9.408	4.547	0.0606	-	-	-	-	-	-	-	-
StableVTON[14]	0.8543	6.439	0.942	0.0905	-	-	-	-	-	-	-	-
LaDI-VTON [17]	0.8603	11.386	7.248	0.0733	14.648	8.754	0.7656	9.555	4.683	0.2366	10.676	5.787
IDM-VTON [3]	0.8499	5.762	0.732	0.0603	9.842	1.123	0.8797	6.821	2.924	0.0563	9.546	4.320
OOTDiffusion [28]	0.8187	9.305	4.086	0.0876	12.408	4.689	0.8854	4.610	0.955	0.0533	12.567	6.627
CatVTON[4]	0.8704	5.425	0.411	0.0565	9.015	1.091	0.8922	3.992	0.818	0.0455	6.137	1.403
Ours	0.8853	5.236	0.401	0.0477	8.627	0.747	0.9237	2.862	0.290	0.0291	4.966	0.961

Table 2. Quantitative comparisons for image Virtual Try-On.



Figure 6. Qualitative comparison on the VIVID dataset.



Figure 7. Ablation study on the VIVID dataset. Top row: “lower body” as text input; bottom row: “upper body” as text input.

Methods	SSIM $\uparrow$	LPIPS $\downarrow$	$FVD_I \downarrow$	$FVD_R \downarrow$
FW-GAN [25]	0.675	0.283	8.019	12.150
ClothFormer [12]	0.921	0.081	3.967	5.048
Tunnel Try-on [30]	0.913	0.054	3.345	4.614
VIVID [5]	0.949	0.068	3.405	5.074
VITON-DiT [36]	0.896	0.080	2.498	0.187
<b>Ours</b>	<b>0.971</b>	<b>0.019</b>	<b>1.926</b>	<b>0.035</b>
VIVID [5]	0.8747	0.0818	1.1394	0.0484
<b>Ours</b>	<b>0.8879</b>	<b>0.0632</b>	<b>0.9237</b>	<b>0.0362</b>

Table 3. Quantitative comparison on the VVT and VIVID datasets.

### 4.3. Comparison with SOTA Methods

For image VTION, we compare with diffusion-based methods, (e.g. DCI-VTON [8], LaDI-VTON [17], IDM-VTON [3], StableVTON [14], OOTDiffusion [28] and CatVTON [4]) as they significantly outperform previous GAN-based methods. For video VTION, we collected several state-of-the-art methods, covering GAN-based methods like FW-GAN [25], ClothFormer [12] and diffusion-based methods like Tunnel Try-on [30], VIVID [5] and VITON-DiT [37].

**Image VTION Comparison** In Fig. 4 and Table. 2, we provide qualitative and quantitative comparisons, respectively. Quantitatively, our methods significantly surpass all SOTA methods by a substantial margin. Qualitatively, our method far surpasses others in maintaining clothing styles, preserving logos, and enriching texture details. For example, in the second row of Fig. 4, it is evident that the logos produced by alternative models often exhibit inaccuracies in color distribution or omit specific details. In contrast, our method demonstrates superior capability in preserving the intricate details of the clothing.

**Video VTION Comparison** As illustrated in Table 3, our method demonstrates substantial advancements over other approaches with respect to the SSIM, LPIPS, and VFID metrics. These improvements underscore the superiority of our approach in maintaining clothing details and ensuring temporal continuity. Figures 5 and 6 present the qualitative results of various methods applied to the VVT and VIVID



Figure 8. Comparison between Masked and Mask-Free VTON datasets, respectively. We can see that earlier video VTON techniques often result in blurred outputs with notable color inconsistencies in the generated clothing. Our method, by contrast, distinctly surpasses these others, excelling in both the preservation of clothing details and ensuring temporal continuity. This is especially evident in its ability to retain text accurately.

#### 4.4. Ablation Study

We conduct extensive ablations on VIVID [5] dataset to verify the effectiveness of each components, and the visual results is reported in Fig. 7.

- (a) and (c): We explore the integration of text and reference garment as a combined condition for normalization, while the features of video are normalized independently. Refer to Fig. 3, our findings indicate that normalizing the text and reference image together tends to gradually diminish the garment features, which in turn significantly impacts the quality of the generated results. In contrast, by concatenating features of the same modality together and then performing normalization, We can achieve a reasonable result.
- (b) and (c): We observe that image-video joint training yields generated clothing that more closely resembles the reference garments. This outcome can be attributed to the substantial volume of image pair data, which significantly enhances the generalization of our method.
- (d), (e) and (f): (d) and (f) are images from a generated video clip at time  $t = 6$ , with resolutions of  $512 \times 384$  and  $832 \times 624$ , respectively. (e) is an image from the clip at time  $t = 33$ . According to Sec. 4.2, through feature fusion and modality-specific normalization, text, reference garment and video can share the same attention layers, which enable us to generate video clips with higher resolution and longer duration.

#### 4.5. User Study

As the same setting as Tunnel Try-on [30], we conducted two user studies involving 100 participants from diverse backgrounds and age groups to objectively assess our methods against the state-of-the-art techniques in image and

Methods	Quality	Fidelity	Smoothness
OOTDiffusion [28]	10%	7%	-
IDM-VTON [3]	12%	14%	-
CatVTON [4]	13%	12%	-
Ours	65%	67%	-
VIVID [5]	32%	25%	8%
Ours	68%	75%	92%

Table 4. User study on preference rates for the VITONHD and VIVID datasets.

video VTON. The evaluation involves three aspects: i) *Quality* denotes the image quality; ii) *Fidelity* evaluates the ability to preserve garment details. iii) *Smoothness* measures the temporal consistency of generated videos. The results indicate that our method considerably outperforms other methods, particularly in terms of video smoothness.

#### 4.6. Application-Parsing Free Virtual Tryon

It’s quite surprising that our method can generate realistic videos, and one piece of evidence is that our method can be used for mask-free video VTON. We found that one of the biggest challenges for mask-free video VTON is the lack of paired video (*e.g.* two identical videos but with different garments), but our method fills this gap. We can use our well-trained MN-VTON to generate paired data, and then proceed with the training of the parsing-free video VTON. As shown in Fig. 8, the effectiveness of masked VTON is highly reliant on the quality of the mask. If there are detection omissions in the mask, achieving accurate generation results becomes challenging. In contrast, mask-free VTON does not suffer from this issue. Additionally, since the mask must fully encompass the clothing area, it often ends up covering regions that do not need alteration (*e.g.* bag, arm). Mask-free VTON effectively avoids this problem.

### 5. Conclusion

In this paper, we proposed a novel single-network approach for virtual try-on (VTON), challenging the need for dual networks to achieve high-quality results. By incorporating a modality-specific normalization strategy, our method efficiently processes and integrates text, image, and video features within a single framework, addressing key challenges in garment realism, texture preservation, and feature alignment. Extensive experiments demonstrate that our method delivers superior visual quality and detail, matching or surpassing dual-network approaches in both resolution and fidelity, while significantly reducing computational overhead. Our work highlights the potential of single-network architectures for scalable, high-performance VTON systems, offering a more efficient solution for real-world applications.



## References

- [1] Junsong Chen, Jincheng Yu, Chongjian Ge, Lewei Yao, Enze Xie, Yue Wu, Zhongdao Wang, James Kwok, Ping Luo, Huchuan Lu, et al. Pixart: Fast training of diffusion transformer for photorealistic text-to-image synthesis. *arXiv preprint arXiv:2310.00426*, 2023. 5
- [2] Seunghwan Choi, Sunghyun Park, Minsoo Lee, and Jaegul Choo. Viton-hd: High-resolution virtual try-on via misalignment-aware normalization. In *Proc. of the IEEE conference on computer vision and pattern recognition (CVPR)*, 2021. 1, 2, 5
- [3] Yisol Choi, Sangkyung Kwak, Kyungmin Lee, Hyungwon Choi, and Jinwoo Shin. Improving diffusion models for authentic virtual try-on in the wild. *arXiv preprint arXiv:2403.05139*, 2024. 2, 3, 7, 8
- [4] Zheng Chong, Xiao Dong, Haoxiang Li, Shiyue Zhang, Wenqing Zhang, Xujie Zhang, Hanqing Zhao, and Xiaodan Liang. Catvton: Concatenation is all you need for virtual try-on with diffusion models, 2024. 3, 7, 8
- [5] Zixun Fang, Wei Zhai, Aimin Su, Hongliang Song, Kai Zhu, Mao Wang, Yu Chen, Zhiheng Liu, Yang Cao, and Zheng-Jun Zha. Vivid: Video virtual try-on using diffusion models. *arXiv preprint arXiv:2405.11794*, 2024. 1, 2, 3, 5, 6, 7, 8
- [6] Yuying Ge, Yibing Song, Ruimao Zhang, Chongjian Ge, Wei Liu, and Ping Luo. Parser-free virtual try-on via distilling appearance flows, 2021. 3
- [7] Ian Goodfellow, Jean Pouget-Abadie, Mehdi Mirza, Bing Xu, David Warde-Farley, Sherjil Ozair, Aaron Courville, and Yoshua Bengio. Generative adversarial nets. *Advances in neural information processing systems*, 27, 2014. 2
- [8] Junhong Gou, Siyu Sun, Jianfu Zhang, Jianlou Si, Chen Qian, and Liqing Zhang. Taming the power of diffusion models for high-quality virtual try-on with appearance flow. In *Proceedings of the 31st ACM International Conference on Multimedia*, pages 7599–7607, 2023. 2, 3, 7
- [9] Xintong Han, Zuxuan Wu, Zhe Wu, Ruichi Yu, and Larry S Davis. Viton: An image-based virtual try-on network. In *CVPR*, 2018. 2, 3
- [10] Li Hu. Animate anyone: Consistent and controllable image-to-video synthesis for character animation. In *Proceedings of the IEEE/CVF Conference on Computer Vision and Pattern Recognition*, pages 8153–8163, 2024. 3
- [11] Li Hu, Xin Gao, Peng Zhang, Ke Sun, Bang Zhang, and Liefeng Bo. Animate anyone: Consistent and controllable image-to-video synthesis for character animation, 2024. 3
- [12] Jianbin Jiang, Tan Wang, He Yan, and Junhui Liu. Clothformer: Taming video virtual try-on in all module. In *Proceedings of the IEEE/CVF Conference on Computer Vision and Pattern Recognition*, pages 10799–10808, 2022. 7
- [13] Jeongho Kim, Gyojung Gu, Minhoo Park, Sunghyun Park, and Jaegul Choo. Stableviton: Learning semantic correspondence with latent diffusion model for virtual try-on, 2023. 3
- [14] Jeongho Kim, Guojung Gu, Minhoo Park, Sunghyun Park, and Jaegul Choo. Stableviton: Learning semantic correspondence with latent diffusion model for virtual try-on. In *Proceedings of the IEEE/CVF Conference on Computer Vision and Pattern Recognition*, pages 8176–8185, 2024. 2, 3, 7
- [15] Sangyun Lee, Gyojung Gu, Sunghyun Park, Seunghwan Choi, and Jaegul Choo. High-resolution virtual try-on with misalignment and occlusion-handled conditions. *arXiv preprint arXiv:2206.14180*, 2022. 2
- [16] Davide Morelli, Matteo Fincato, Marcella Cornia, Federico Landi, Fabio Cesari, and Rita Cucchiara. Dress Code: High-Resolution Multi-Category Virtual Try-On. In *Proceedings of the European Conference on Computer Vision*, 2022. 2, 5
- [17] Davide Morelli, Alberto Baldrati, Giuseppe Cartella, Marcella Cornia, Marco Bertini, and Rita Cucchiara. LaDIVTON: Latent Diffusion Textual-Inversion Enhanced Virtual Try-On. In *Proceedings of the ACM International Conference on Multimedia*, 2023. 2, 3, 4, 7
- [18] Davide Morelli, Alberto Baldrati, Giuseppe Cartella, Marcella Cornia, Marco Bertini, and Rita Cucchiara. Ladi-vton: Latent diffusion textual-inversion enhanced virtual try-on, 2023. 3
- [19] Taesung Park, Ming-Yu Liu, Ting-Chun Wang, and Jun-Yan Zhu. Semantic image synthesis with spatially-adaptive normalization. In *Proceedings of the IEEE/CVF conference on computer vision and pattern recognition*, pages 2337–2346, 2019. 2, 3, 4
- [20] William Peebles and Saining Xie. Scalable diffusion models with transformers, 2023. 3
- [21] Alec Radford, Jong Wook Kim, Chris Hallacy, Aditya Ramesh, Gabriel Goh, Sandhini Agarwal, Girish Sastry, Amanda Askell, Pamela Mishkin, Jack Clark, et al. Learning transferable visual models from natural language supervision. In *International conference on machine learning*, pages 8748–8763. PMLR, 2021. 2
- [22] Ke Sun, Jian Cao, Qi Wang, Linrui Tian, Xindi Zhang, Lian Zhuo, Bang Zhang, Liefeng Bo, Wenbo Zhou, Weiming Zhang, and Daiheng Gao. Outfitanyone: Ultra-high quality virtual try-on for any clothing and any person, 2024. 3
- [23] Bochao Wang, Huabin Zheng, Xiaodan Liang, Yimin Chen, and Liang Lin. Toward characteristic-preserving image-based virtual try-on network. In *Proceedings of the European Conference on Computer Vision (ECCV)*, pages 589–604, 2018. 2
- [24] Bochao Wang, Huabin Zheng, Xiaodan Liang, Yimin Chen, Liang Lin, and Meng Yang. Toward characteristic-preserving image-based virtual try-on network, 2018. 3
- [25] Junjun Wu, Xilin Liu, Qinghua Lu, Zeqin Lin, Ningwei Qin, and Qingwu Shi. Fw-gan: Underwater image enhancement using generative adversarial network with multi-scale fusion. *Signal Processing: Image Communication*, 109: 116855, 2022. 2, 5, 6, 7
- [26] Zhenyu Xie, Zaiyu Huang, Fuwei Zhao, Haoye Dong, Michael Kampffmeyer, and Xiaodan Liang. Towards scalable unpaired virtual try-on via patch-routed spatially-adaptive gan. *Advances in Neural Information Processing Systems*, 34:2598–2610, 2021. 2
- [27] Zhenyu Xie, Zaiyu Huang, Xin Dong, Fuwei Zhao, Haoye Dong, Xijin Zhang, Feida Zhu, and Xiaodan Liang. Gp-vton: Towards general purpose virtual try-on via collaborative local-flow global-parsing learning, 2023. 3

- [28] Yuhao Xu, Tao Gu, Weifeng Chen, and Chengcai Chen. Oot-diffusion: Outfitting fusion based latent diffusion for controllable virtual try-on. *arXiv preprint arXiv:2403.01779*, 2024. [2](#), [3](#), [5](#), [7](#), [8](#)
- [29] Yuhao Xu, Tao Gu, Weifeng Chen, and Chengcai Chen. Oot-diffusion: Outfitting fusion based latent diffusion for controllable virtual try-on, 2024. [3](#)
- [30] Zhengze Xu, Mengting Chen, Zhao Wang, Linyu Xing, Zhonghua Zhai, Nong Sang, Jinsong Lan, Shuai Xiao, and Changxin Gao. Tunnel try-on: Excavating spatial-temporal tunnels for high-quality virtual try-on in videos. *arXiv preprint arXiv:2404.17571*, 2024. [2](#), [3](#), [7](#), [8](#)
- [31] xujie zhang, Xiu Li, Michael Kampffmeyer, Xin Dong, Zhenyu Xie, Feida Zhu, Haoye Dong, and Xiaodan Liang. Warpdiffusion: Efficient diffusion model for high-fidelity virtual try-on, 2023. [3](#)
- [32] Zhuoyi Yang, Jiayan Teng, Wendi Zheng, Ming Ding, Shiyu Huang, Jiazheng Xu, Yuanming Yang, Wenyi Hong, Xiaohan Zhang, Guanyu Feng, et al. Cogvideox: Text-to-video diffusion models with an expert transformer. *arXiv preprint arXiv:2408.06072*, 2024. [3](#), [5](#)
- [33] Xujie Zhang, Ente Lin, Xiu Li, Yuxuan Luo, Michael Kampffmeyer, Xin Dong, and Xiaodan Liang. Mmtryon: Multi-modal multi-reference control for high-quality fashion generation. *arXiv preprint arXiv:2405.00448*, 2024. [2](#), [3](#)
- [34] Xujie Zhang, Ente Lin, Xiu Li, Yuxuan Luo, Michael Kampffmeyer, Xin Dong, and Xiaodan Liang. Mmtryon: Multi-modal multi-reference control for high-quality fashion generation, 2024. [3](#)
- [35] Fuwei Zhao, Zhenyu Xie, Michael Kampffmeyer, Haoye Dong, Songfang Han, Tianxiang Zheng, Tao Zhang, and Xiaodan Liang. M3d-vton: A monocular-to-3d virtual try-on network. In *Proceedings of the IEEE/CVF International Conference on Computer Vision*, pages 13239–13249, 2021. [2](#)
- [36] Jun Zheng, Fuwei Zhao, Youjiang Xu, Xin Dong, and Xiaodan Liang. Viton-dit: Learning in-the-wild video try-on from human dance videos via diffusion transformers. *arXiv preprint arXiv:2405.18326*, 2024. [2](#), [7](#)
- [37] Jun Zheng, Fuwei Zhao, Youjiang Xu, Xin Dong, and Xiaodan Liang. Viton-dit: Learning in-the-wild video try-on from human dance videos via diffusion transformers, 2024. [3](#), [7](#)
- [38] Zangwei Zheng, Xiangyu Peng, Tianji Yang, Chenhui Shen, Shenggui Li, Hongxin Liu, Yukun Zhou, Tianyi Li, and Yang You. Open-sora: Democratizing efficient video production for all, 2024. [3](#)
- [39] Xie Zhenyu, Huang Zaiyu, Dong Xin, Zhao Fuwei, Dong Haoye, Zhang Xijin, Zhu Feida, and Liang Xiaodan. Gp-vton: Towards general purpose virtual try-on via collaborative local-flow global-parsing learning. In *Proceedings of the IEEE/CVF Conference on Computer Vision and Pattern Recognition (CVPR)*, 2023. [2](#), [3](#)
- [40] Luyang Zhu, Dawei Yang, Tyler Zhu, Fitsum Reda, William Chan, Chitwan Saharia, Mohammad Norouzi, and Ira Kemelmacher-Shlizerman. Tryondiffusion: A tale of two unets, 2023. [2](#), [3](#)
- [41] Luyang Zhu, Yingwei Li, Nan Liu, Hao Peng, Dawei Yang, and Ira Kemelmacher-Shlizerman. M&m vto: Multi-garment virtual try-on and editing. In *Proceedings of the IEEE/CVF Conference on Computer Vision and Pattern Recognition*, pages 1346–1356, 2024. [2](#)